

The effects of time correlations in subcritical fracture. An acoustic analysis

M. Stojanova^a, S. Santucci^b, L. Vanel^a, O. Ramos^a

a. *Institut Lumière Matière, UMR5306 Université Lyon 1-CNRS, Université de Lyon 69622
Villeurbanne cedex, France.*

b. *Laboratoire de Physique, CNRS UMR 5672, Ecole Normale Supérieure de Lyon, Université de
Lyon, 46 allée d'Italie, 69364 Lyon Cedex 07, France.*

Résumé :

Nous avons étudié les émissions acoustiques résultant de la rupture sous-critique d'une feuille de papier. La fracture avance par des sauts discrets produisant des événements acoustiques soudains et discrets. Le temps d'attente entre deux événements acoustiques et l'énergie des événements sont distribués suivant des lois de puissance. La valeur de l'exposant de la loi de puissance pour la distribution des énergies dépend fortement de la fréquence de l'analyse. Cet effet est dû aux corrélations temporelles entre les événements et en particulier à l'existence de répliques.

Abstract :

The acoustic emissions resulting from the subcritical fracture of a sheet of paper are analyzed. A single crack advances through a series of discrete fracture jumps resulting in discrete acoustic burst-like events. Both the waiting time between consecutive events and the energy of the bursts are distributed according to power laws. Surprisingly, the exponent value of the power law for the energy distribution strongly depends on the frequency of the analysis. This effect is provoked by temporal correlations between the events, in particular by the presence of aftershocks.

Mots clefs : subcritical fracture ; aftershocks ; critical exponents

1 Introduction

It is well known that there is a critical value for a load that a brittle structure can hold without quasi-instantaneously breaking into pieces. However, even a subcritical load can provoke the failure of a structure, but in a time-dependent manner. As stresses intensify around a flaw in the material [5], a micro-crack can start growing, in an intermittent manner (the case of heterogeneous materials), until reaching a critical length where the whole system fails. This process, denominated *subcritical fracture* [4, 10, 13, 17], belongs to a large family of “catastrophic” phenomena evolving through discrete, power law distributed events whose best-known example are earthquakes [2, 6, 12]. Predicting large events is the ultimate goal concerning these systems. However, most of the theoretical approaches explaining their dynamics have been exploited by the formalism of critical phenomena, which invalidates predictability and is ruled by universality classes [1, 15]. This classification into universality classes is based on the consideration of characteristic exponent values for different power laws describing the dynamics of the system. In contradiction with these ideas, recent experiments show exponents which are sensitive to material properties [3]. The possibility of predicting large events has also been explored [11].

In this work, the acoustic emissions resulting from the subcritical fracture of a sheet of paper containing a crack and submitted to a constant force are analyzed. The distribution of the events' energies follows a power law distribution, with exponents that, surprisingly, depend on the frequency of the analysis. We

show that this effect is provoked by time correlations between events, in particular, by the presence of aftershocks (which are common in this family of catastrophic phenomena). The distribution of waiting time between consecutive events also follows a power law distribution. However its exponent is not affected by the frequency of the analysis.

2 Experimental procedure

We use fax paper samples from Alrey having a thickness of $50 \mu m$ and effective dimensions $21 cm \times 4 cm$, being fixed along the longer sides and free in the perpendicular direction. An initial crack of length l_0 is prepared at one free side of the sample, both in a parallel direction and equidistant from the fixed borders. Experiments are performed by applying a constant force F perpendicularly to the direction of the initial crack. By adjusting $l_0 = 4.75 cm$ and $F = 200 N$, the crack grows reaching a critical length, $l_c \sim 8 cm$, in approximately 10 to 30 minutes after the application of the force. The critical length l_c separates the slow dynamics from the quasi-instantaneous rupture. A piezoelectric transducer of diameter $2.3 mm$ (*Valpey Fisher VP-1.5*) is placed in contact with the paper at $5 cm$ from the free side containing the initial crack and at $1 cm$ from the fixed border (which also corresponds to a $1 cm$ distance to the direction of the initial crack). An ultrasonic gel guarantees a good contact between the sensor and the sheet of paper. The acoustic signals are amplified by $64 dB$ and recorded continuously during the whole experience by a *NI USB-6366* card at $2 MHz$. All experiences have been performed under the same conditions. The temperature and relative humidity were $26.5 \pm 1^\circ C$ and $45 \pm 2\%$ respectively.

The amplitude of the acoustic signal depends on the contact between the transducer and the sheet of paper, which varies between different realizations. In order to compare events from different experiences, a calibration was performed. It consisted on the averaged response of each sensor to six localized rupture events produced on every sample (by piercing it with a computer controlled thin needle of $250 \mu m$ of diameter) before complete loading. Additional series of experiments was done in order to study the attenuation of acoustic waves in paper. 10 to 20 localized rupture events were induced on a sheet of paper submitted to a force of $200 N$, but with no initial crack to limit spontaneous and uncontrolled rupture events. The events were made on a line parallel to the longer sides of the paper, in the same direction as the fracture in previous experiments. The acoustic signal was recorded by two sensors placed at $4 cm$ from each-other.

In addition to the acoustic measurements, a high-speed camera (*Photron FASTCAM SA4*) recorded images in a rectangular area containing the advancing crack at a frequency of $10 Hz$ and a spatial resolution of $100 \mu m/pixel$.

2.1 Data Analysis

To detect acoustic events we use spectral distance calculation. Usually spectral distance calculation is done by considering the logarithms of the power spectra of signals. We choose to define a linear spectral distance which is directly proportional to the signal's energy and thus makes energy estimations simpler. Spectral distance is calculated as the integral over a time window (w) of the difference between the power spectra of the signal averaged over all the frequencies ($\langle S(t) \rangle$) and the power spectra of the noise, averaged over all the frequencies and over a time interval of at least $0.5s$ ($\langle \bar{N} \rangle$) :

$$D_{S,N}(t) = \frac{1}{w} \int_{t-\frac{w}{2}}^{t+\frac{w}{2}} (\langle S(t') \rangle - \langle \bar{N} \rangle) dt' \quad (1)$$

We choose a time interval of $w = 100 \mu s$ which is slightly greater than the duration of the shortest acoustic events. Noise power spectrum is determined using the signal recorded during the calibration, for which no uncontrolled rupture has occurred. We detect acoustic events by thresholding the spectral distance. The threshold is defined as the maximum value of the spectral distance of the noise with itself : $trsh = max(D_{N,N}(t))$.

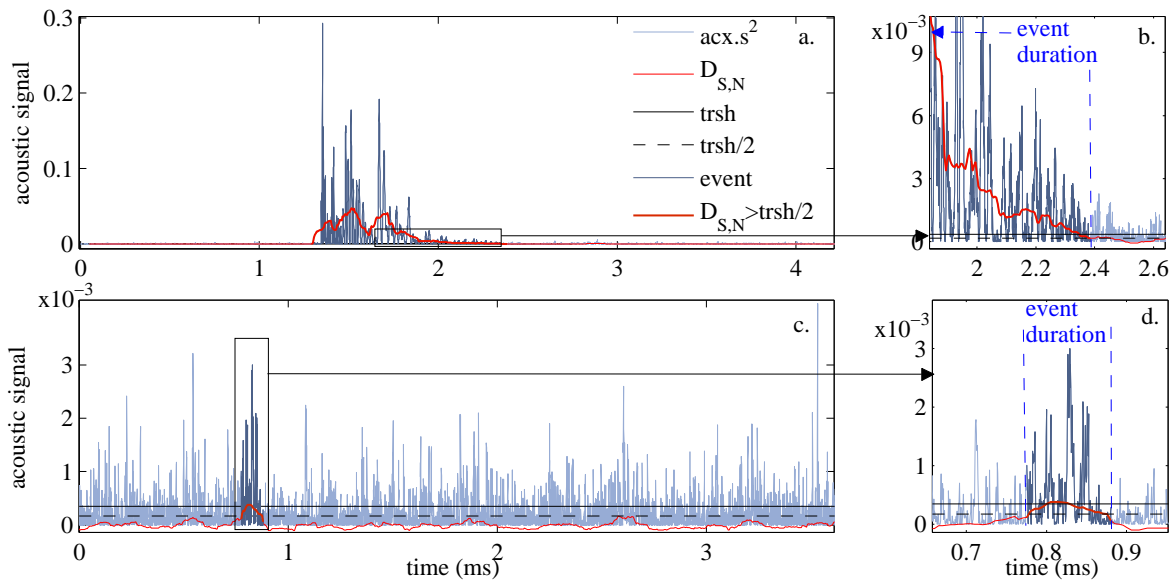


FIGURE 1 – Detection of acoustic events. Light blue line ($acx.s^2$) : square of the acoustic signal, thin red line ($D_{S,N}$) : spectral distance of the signal to the noise, black line ($trsh$) : threshold value of the spectral distance, black dashed line ($trsh/2$), dark gray line ($event$) : acoustic signal corresponding to an event, thick dark red line ($D_{S,N} > trsh/2$) : spectral distance over the event's duration (a) High energy event : the acoustic event presents few maxima. (b) Determining the end of an event by thresholding the spectral distance. (c) Low energy event : the event's amplitude is in the range of the noise amplitude. (d) Zoom on the low energy event.

This method is much more sensitive to acoustic emissions in paper compared to signal thresholding : in our case the number of events detected is almost four times greater. It is possible to detect events whose amplitude is in the range of the noise amplitude (figure 1 c and d).

The energy of acoustic events is defined as the integral of the spectral distance (equation 1) over an event's duration. Once an event is detected using the initial threshold, it's duration is defined as the part of the spectral distance overcoming the threshold divided by 2. We prefer this definition of the energy to the maximal amplitude of the signal (or of the spectral distance) because acoustic events are not single punctual bursts : they sometimes have irregular shapes in time, presenting few local maxima as consequence of the fact that few fibers can break consecutively in a very small lapse of time, appearing as one single event (figure 1.a). Taking into account only one of these maxima would result in neglecting a considerable proportion of the acoustic energy. Integrating the spectral distance rather than the square of the signal itself decreases the influence of the noise.

3 Results

As the applied force is subcritical and the material heterogeneous, the initial crack propagates in an intermittent manner [13] : images show that the length of the fracture is constant for most of the time and increases by making fast discrete crack steps denominated *jumps* or *avalanches* [16]. The acoustic data shows discrete *bursts* with a finite duration. Each burst constitutes an acoustic event. The analysis focuses on the distribution of waiting times between events and the distribution of events' energies ; and in particular their dependence on the frequency of the analysis. This is quite relevant when comparing different measurements taken at different frequencies. In our case, the acoustic sampling is performed at 2 MHz while the frame rate of the images corresponds to 10 Hz. The changing in frequency has been performed numerically, by dividing the time series in equispaced intervals of duration δt and adding all the energies of the events belonging to the interval. δt has been chosen between $10^{-4}s$ (smallest waiting time value) and 0.5s. For δt below $10^{-4}s$ the result we obtain doesn't vary from the one obtained without changing the frequency ; if δt is smaller than the smallest waiting

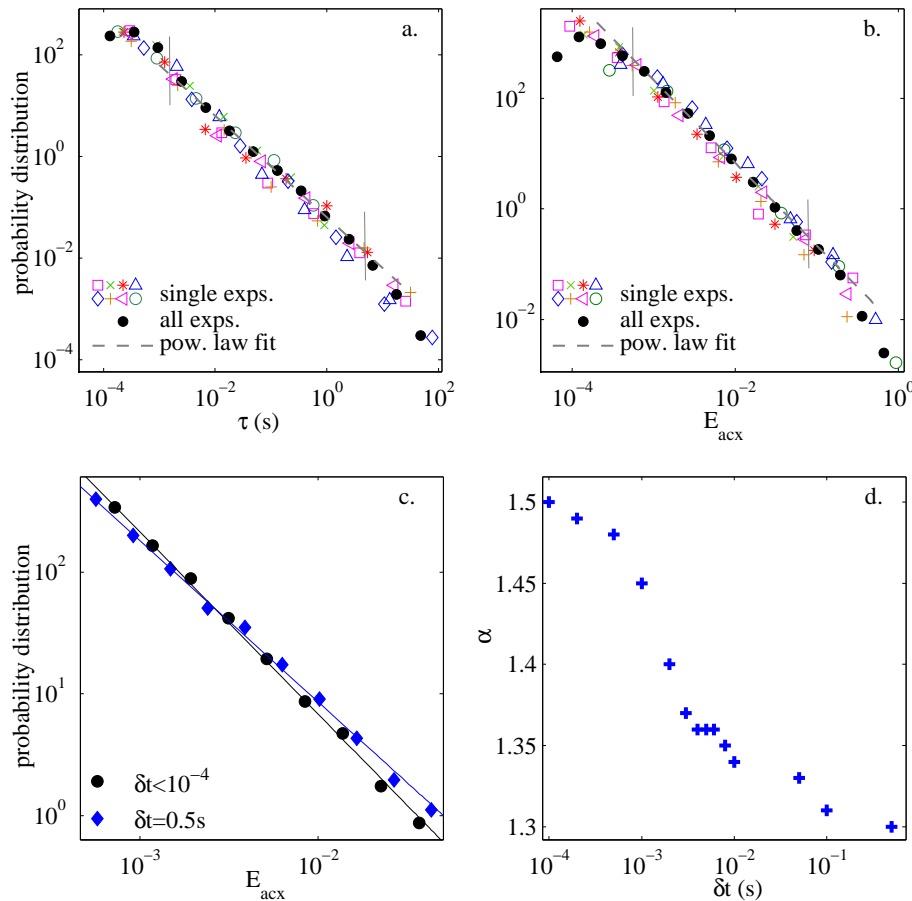


FIGURE 2 – (a) Distributions of waiting times between events ($\delta t < 10^{-4}$). (b) Distribution of the events' energies ($\delta t < 10^{-4}$). Open symbols : of each experiment separately, solid symbols : ensemble average of all experiments, dashed line : power law fits of the ensemble average in the signalized range. (c) Distributions of the energy for the minimal and maximal δt values considered, within the fitting range. (d) Exponents of the power law distributions of the energy as a function of δt .

time between events, each time interval contains at most one single event and the energy distribution remains unchanged.

Waiting Times : For subcritical fractures the time between two discrete events, referred to as the waiting time, follows power law distributions [3, 7, 14]. Figure 2a shows the probability distribution of waiting times between the events for the acoustic data (at $\delta t = 10^{-4}$ s). The distribution is fitted as a power law $P(\tau) \sim \tau^{-\beta}$ with an exponent $\beta = 1.00 \pm 0.03$. As δt changes from 10^{-4} s to 1s the distributions move to higher τ values, but their exponent β remains constant.

Energies : The spectral distance integration provides an estimation of the acoustic energy detected by the sensors, which does not exactly correspond to the energy at the event's source. This energy needs to be corrected by taking into account the attenuation of the acoustic waves, which can be scattered or absorbed by paper fibers. If acoustic events are uniformly distributed in the sample, the power law exponent can be independent of wave attenuation [18], else the distribution of the acoustic energy will be affected by the attenuation [8]. In our experiments acoustic events are localized along the fracture line, so attenuation should be taken into account. Experiments on crack-free paper provided data on the position and energy of about hundred events relative to the two different sensors. By comparing the energy ratio of signals detected by the two sensors to the distance separating each event from the sensors, we obtained that the energy is attenuated following $E(r)/E_s \sim (1/r)\exp(-r/r_c)$, where E_s corresponds to the energy at the source ($r = 0$) and r_0 is a characteristic length equal to 11.1 cm. To determine the position of the source of an acoustic event we use the images and suppose that

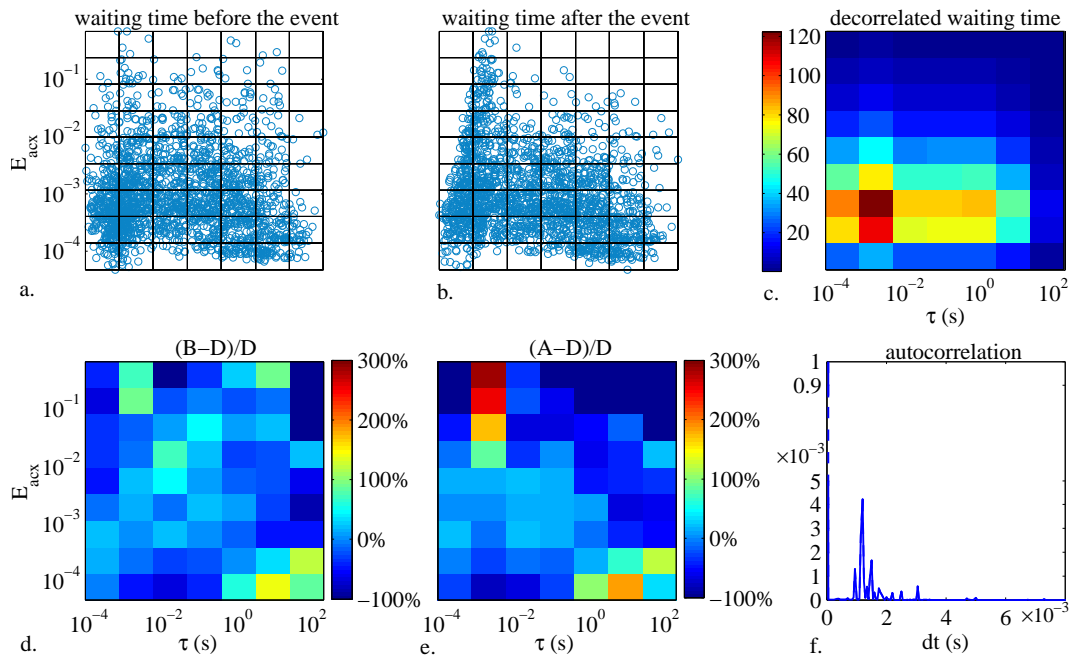


FIGURE 3 – (a) Repartition of events’ energies and waiting times before events. (b) Repartition of events’ energies and waiting times after events. (c) Repartition of events’ energies and mixed-up waiting times. (d) Relative difference between the number of events in each interval for waiting times before the event and uncorrelated waiting times. (e) Relative difference between the number of events in each interval for waiting times after the event and uncorrelated waiting times. (f) Temporal autocorrelation of the acoustic signal.

it occurred at the position of the crack tip at the corresponding time. By knowing the distance between the source and the sensor, we can compute the attenuation of the energy. The estimated acoustic energy at the event’s source (figure 2b) follows a power law $P(E) \sim E^{-\alpha}$ with an exponent of $\alpha = 1.51 \pm 0.06$ (without considering the wave attenuation the exponent is of 1.55 ± 0.03). As δt increases, the distribution of the acoustic energy still follows a power law, but its exponent α is strongly affected (figures 2c, d).

If energy and waiting time distributions were uncorrelated, calculating the energy for different time intervals (i.e., at different frequencies) should only change the range of energies without affecting the exponent of the power law distribution. Thus, the strong dependence shown in figure 2d indicates that there may exist a correlation between the waiting time and the energy of an event. To identify it we study waiting times and energies of the events of all experiments combined.

On figure 3 we represented each event by a point on a energy-waiting time diagram. Each event is defined by its energy and can be represented with the waiting time that precedes it (a) or the waiting time that follows it (b). We can see on (b) that there is a large density of events for large energies (top) and small waiting times (left). To compare this to a case where waiting times and energies are uncorrelated, we considered a case where a random waiting time from the experiments is associated to each event (c). The three diagrams were divided in 7×9 cells, and the number of events in each cell is stored in 7×9 matrices : B for waiting times before the events, A for waiting times after the events, and D for the uncorrelated waiting time. For more accuracy the matrix D was calculated as the mean of the distribution of 1000 random energy-waiting time redistributions. Finally, a comparison between experimental results (A and B) and the uncorrelated case (D) is made by calculating the relative difference between the matrices. The result is shown on figure 3 d, e. As expected, the number of events having large energy and followed by small waiting times is much larger for the experimental data than for the uncorrelated case (e). On the other hand, this behavior is not observed for waiting times preceding the events. This shows the existence of aftershocks during the propagation of the crack,

with typical waiting time of 10^{-3} s, corroborated by the analysis of the temporal autocorrelation of the signal, considering a $\delta t = 10^{-4}$ s (figure 3f). A time of about 10^{-3} s also corresponds to the maximal variation of the energy distribution exponent (figure 2d) confirming that the dependence of the exponent on the signal's frequency is due to the aftershocks. Also, for both waiting times (before and after the event) we observe a large density for small energies (bottom right of d and e), meaning that there exist "inactivity times" characterized by long waiting times and low energy events.

4 Conclusions

We studied the subcritical crack growth of a single crack in a sheet of paper submitted to a constant force by using acoustic emissions as the main source of information. Direct image analysis was also performed. Two variables, the waiting times between the events and the energy released at each event, were statistically analyzed. They both present power law distributions. The exponent of the power law for the waiting time distribution is quite robust to variations in the frequency of the analysis. However, the corresponding exponent for the energy distribution shows a strong dependence with frequency. This effect is provoked by time correlations between events, in particular, by the presence of aftershocks. Considering that aftershocks are a common feature of many different phenomena evolving through power law distributed events, this effect can be relevant to a large family of phenomena.

We acknowledge financial support from the Federation of Research "A. M. Ampère" of Lyon (FRAMA).

Références

- [1] Barabasi, A.L. Stanley, H.E. 1995 *Fractal Concepts in Surface Growth* Cambridge Univ. Press, New York.
- [2] Baró, J., et al. 2013 *Phys. Rev. Lett.* **110** 088702.
- [3] Deschanel, S., Vanel, L., Godin, N., Vigier, G., Ciliberto, S., 2009 *J. Stat. Mech.* 01018.
- [4] Garcimartín, A., Guarino, A., Bellon, L., Ciliberto, S., 1997 *Phys. Rev. Lett.* **79** 3202.
- [5] Griffith, A.A. 1920 *Philos. Trans. R. Soc. London, Ser. A.* **221** 163.
- [6] Jensen, H. J. 1998 *Self-organized Criticality, Emergent Complex Behavior in Physical and Biological Systems* Cambridge Univ. Press, Cambridge.
- [7] Kun, F., Halász, Z., Andrade Jr, J. S., Herrmann, H. J., 2009 *J. Stat. Mech.* 01021.
- [8] Lavrov, A.V., 2005 *Acoust. Phys.* **51** 3, 383.
- [9] Måløy, K.J., Santucci, S., Schmittbuhl, J., Toussaint, R., 2006 *Phys. Rev. Lett.* **96** 045501.
- [10] Petri, A., Papro, G., Vespignani, A., Alippi, A., Constantini, M., 1994 *Phys. Rev. Lett.* **73** 3423.
- [11] Ramos, O., Altshuler, E., Måløy, K.J., 2009 *Phys. Rev. Lett.* **102** 078701.
- [12] Ramos, O., 2011 Scale invariant avalanches : a critical confusion. in *Horizons in Earth Science Research. Vol. 3 (ed. B.Veress and J.Szigethy)* pp. 157-188, Nova Science, New York.
- [13] Santucci, S., Vanel, L., Ciliberto, S., 2004 *Phys. Rev. Lett.* **93** 095505.
- [14] Santucci, S., Vanel, L., Ciliberto, S., 2007 *Eur. Phys. J. Special Topics* **146** 341.
- [15] Stanley, H.E. 1987 *Introduction to Phase Transitions and Critical Phenomena* Oxford Univ. Press, New York.
- [16] Stojanova, M., Santucci, S., Vanel, L., Ramos, O., 2013 Acoustic emissions in fracturing paper. *13th International Conference on fracture* Beijing.
- [17] Vanel, L., Ciliberto, S., Cortet, P.-P., Santucci, S., 2009 *J. Phys. D : Appl. Phys.* **42** 214007.
- [18] Weiss, J., 1997 *Bull. Seism. Soc. Am.* **87** 5, 1362.